Molecular Cell, Vol. 6, 961–967, October, 2000, Copyright ©2000 by Cell Press

Identification of Paracaspases and Metacaspases: Two Ancient Families of Caspase-like Proteins, One of which Plays a Key Role in MALT Lymphoma

Anthony G. Uren,* Karen O'Rourke,* L. Aravind,† M. Teresa Pisabarro,* Somasekar Seshagiri,* Eugene V. Koonin,† and Vishva M. Dixit*‡
*Genentech Inc.
1 DNA Way
South San Francisco, California 94080
†National Center for Biotechnology Information
National Library of Medicine
National Institutes of Health
Bethesda, Maryland 20894

Summary

Caspases are cysteine proteases essential to apoptosis. We have identified two families of caspase-like proteins, Paracaspases (found in metazoans and *Dictyostelium*) and metacaspases (found in plants, fungi, and protozoa). Metazoan paracaspase prodomains contain a death domain and immunoglobulin domains. Several plant metacaspase prodomains contain zinc finger motifs resembling those in the plant hypersensitive response/cell death protein lsd-1. The human paracaspase prodomain binds Bcl10, a protein involved in the t(1;14)(p22;q32) translocation of mucosa-associated lymphoid tissue (MALT) lymphoma. Another MALT lymphoma translocation, t(11;18)(q21;q21), fuses the *IAP-2* gene to the *MLT1/MALT1* locus, which encodes the human paracaspase. We find that this fusion activates NF-κB and that the caspase domain is required for this function, since mutation of the conserved catalytic cysteine attenuates NF-κB activation.

Introduction

Caspases are a conserved family of central effector proteases considered essential for almost all forms of metazoan programmed cell death. They take their name from their property of being cysteine proteases, the substrates of which have an aspartic acid residue immediately N-terminal to the scissile bond (i.e., an aspartate in the P_1 position) (reviewed in Cohen, 1997). The first identified member of this family, interleukin-1β converting enzyme (ICE/caspase 1), was isolated for its role in IL-1β processing, but subsequently caspases have been shown to be crucial for the regulation of cell death in *C. elegans*, *Drosophila*, and mammals. To date, however, no caspase-like proteases have been identified in plants, fungi, protists, or prokaryotes.

Caspases are synthesized as inactive zymogens that require proteolytic autoprocessing or cleavage by other caspases to generate the catalytically active p20/p10 heterodimer. At their N terminus, a number of caspase zymogens possess large prodomains that encompass protein–protein interaction modules such as the caspase recruitment domain (CARD) and death effector domain (DED). These modules within the prodomain are responsible for specific recruitment of caspases to different cell death–signaling pathways.

The structure of the active forms of caspases 1, 3, and 8 have been solved by X-ray crystallography in complex with peptide inhibitors. The active site is in part comprised of a conserved Cys-His catalytic diad, the cysteine being the active site nucleophile. The aspartate specificity of caspases is determined by conserved basic residues that form the "specificity pocket" that coordinates the substrate's P1 aspartate residue. More recently, the structure of gingipain R, a secreted cysteine protease from the bacterium *Porphyromonas gingivalis*, has also been solved by X-ray crystallography (Protein Data Bank ID code 1CVR). Notably, gingipain R was found to have a similar overall fold to caspases, suggesting an ancient origin for this family of cysteine proteases (Eichinger et al., 1999).

Previous database searches have identified several sequences with distant but statistically significant similarity to caspases (Aravind et al., 1999). These included a human EST (899,640), a predicted ORF from a *C. elegans* (F22D3.6), and an EST sequence from *Dictyostelium discoideum* (gi|3074121). Using full- length sequences of these proteins in further iterative database searches, we were able to distinguish two families of caspase-like proteins, one from animals and slime mold and the other from plants, fungi, and protozoa. We have designated these families paracaspases and metacaspases, respectively. We find that the human paracaspase may play a central role in mucosa-associated lymphoid tissue lymphoma (MALT lymphoma) by its interaction with the *Bcl10* oncogene and through enforced activation of NF-κB signaling.

Results

Identification, Cloning, and Comparison of Paracaspases and Metacaspases

We obtained and sequenced full-length cDNAs corresponding to the novel caspase-like *Homo sapiens* EST, the *Dictyostelium discoideum* EST, and the *Caenorhabditis elegans* genomic sequences (Morio et al., 1998; Aravind et al., 1999). A zebrafish homolog of these genes was also identified and cloned (GenBank accession number AI558594). Using the caspase-like domain of the *Dictyostelium* sequence as a query for a PSI-BLAST search, we identified another, even more distantly related family of caspase-like proteins, members of which are present in *Arabidopsis thaliana* ($e = 10^{-3}$, 5 iterations) and several other plant species, the yeast *Saccharomyces cerevisiae* ($e = 10^{-3}$, 4 iterations) and several other fungi, and in the apicomplexan protist *Plasmodium falciparum* (Figure 1a). Using these novel sequences for iterative searches with the PSI-BLAST program, predicted caspase-type proteases most closely related to metacaspases were also identified in multiple bacterial species,

‡To whom correspondence should be addressed (e-mail: dixit@gene.com).

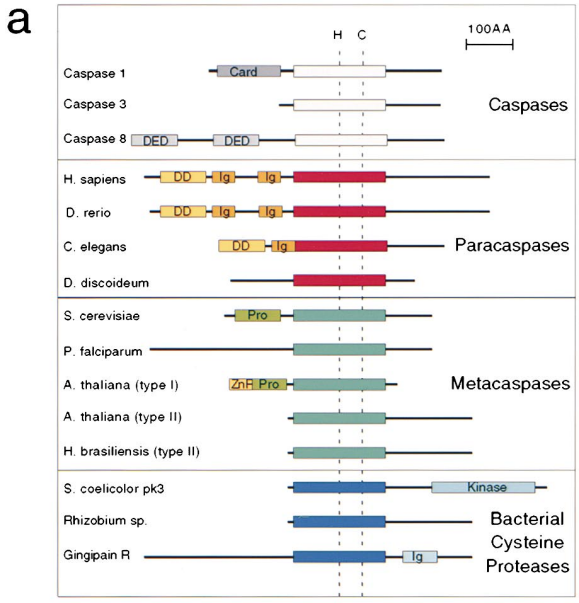

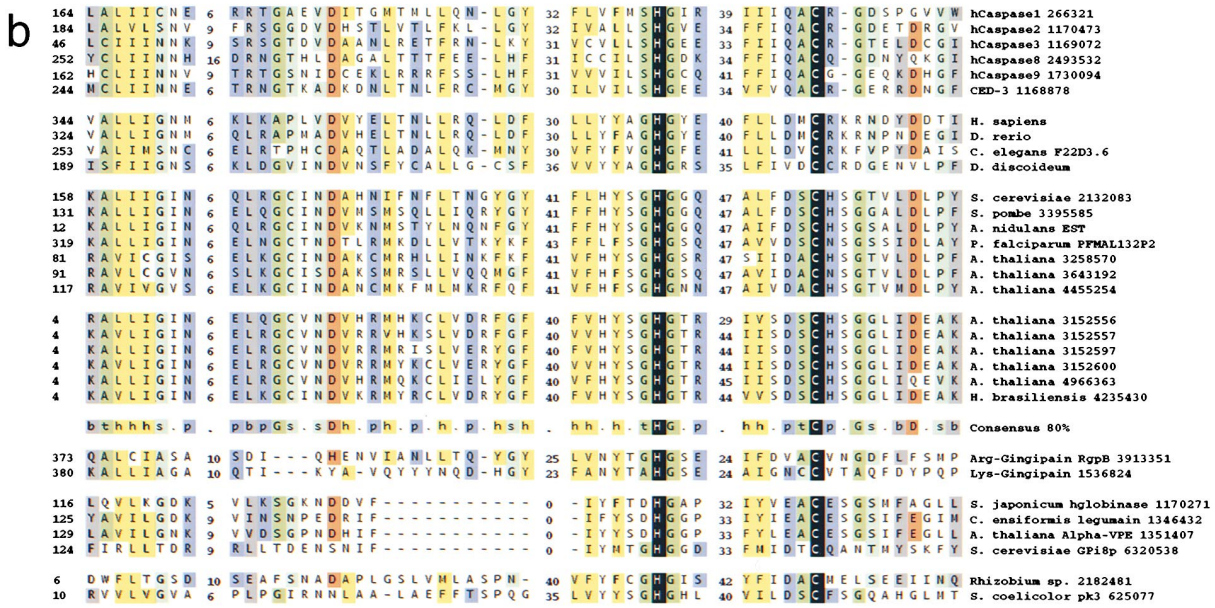

Figure 1. Paracaspases and Metacaspases are Two Novel Families of Caspase-Related Proteins

(a) Domain structure of caspases, paracaspases, and metacaspases. Traditional caspases contain a C-terminal caspase domain (empty box) and in some cases a prodomain with CARD or DED oligomerization motifs. Paracaspases, metacaspases, and a number of bacterial cysteine proteases also contain a predicted caspase-like proteolytic domain. Metazoan paracaspase prodomains encode a death domain ("DD") and either one or two Ig domains. Metacaspases fall into two classes, type I and type II, based on overall structure and the level of sequence similarity. Type I metacaspases from fungi and plants have prodomains with a proline-rich repeat motif ("Pro"). Plant type I metacaspases also have a zinc finger motif ("Zn") similar to those of the plant hypersensitive response protein lsd-1. Type II metacaspases (in plants) have no prodomain but an insertion of approximately 200 amino acids directly C-terminal to their p20-like subunit. pk3, a protein from *Streptomyces coelicolor,* contains a caspase-like domain and a protein kinase domain. Rhizobium sp. plasmid also encodes a caspase-like protein. Gingipain R has a caspase-like catalytic domain (empty box) followed by an Ig-like domain. All sequences are represented as their unprocessed zymogen forms.

(b) Alignment of the p20 subunits of caspases, paracaspases, and metacaspases. From top to bottom the sequences are grouped as caspases, paracaspases, type I metacaspases, type II metacaspases, gingipains, miscellaneous eukaryotic cysteine proteases, and miscellaneous bacterial cysteine proteases. The 80% consensus is compiled from the caspase, paracaspase, and metacaspase sequences. Residues matching the 80% consensus are shaded as follows: hydrophobic (h, yellow); polar (p, blue); charged (c, red); tiny (t, dark green); small (s, light green); big (b, gray). The Cys-His catalytic diad is shaded black.

including *Streptomyces* and *Rhizobium*, *Anabaena*, *Bordetella*, *Geosulfurococcus*, *Rhodosphaera*, *Dehalococcoides*, *Xylella*, and *Synechocystis*.

In Figure 1b, the caspase-related sequences were aligned with the caspase domains of a representative sample of traditional caspases (caspases 1, 2, 3, 8, 9,

and *C. elegans* CED3). Present within all these novel sequences is the universally conserved catalytic cysteine and histidine diad required for catalysis by cysteine proteases. Based on domain structure and sequence similarity, the metazoan and *Dictyostelium* sequences together define a family of predicted proteases that we termed paracaspases. The plant, fungal, and plasmodial sequences form a separate family we have termed metacaspases. These two families, along with the classic caspases and the divergent bacterial members, form a distinct subgroup of a large class of thiol proteases. This class additionally includes legumains, hemoglobinases, and bacterial gingipain R, which has been recently shown to belong to the caspase fold (Chen et al., 1998; Eichinger et al., 1999) (L. A. and E. V. K., unpublished data).

A 3D model of the "caspase-like domain" of human paracaspase has been built based on sequence similarity, secondary structure predictions, threading, and homology modeling approaches (see supplemental data at www.molecule.org/cgi/content/full/6/4/961/DC1). Visual inspection of the residues at the active site of caspase-1, caspase-3, and gingipain R and comparison with those in the paracaspase model provide structural suggestions for substrate-recognition differences, suggesting that, unlike caspases, paracaspases and metacaspases may show specificity toward uncharged residues in the substrate P1 position.

A spectrum of conserved domains is also present in paracaspases and metacaspases outside their caspase-related portions (outlined in Figure 1a). Traditional caspases, in addition to their caspase domain, possess N-terminal prodomains encoding homotypic interaction modules such as CARDs or DEDs. The prodomains of paracaspases from humans, zebrafish, and *C. elegans* contain a death domain (DD) followed by either one or two immunoglobulin (Ig) domains (note: the predicted orf from the *C. elegans* genome project sequence, FD223.6, lacks this death domain due to a frameshift that is absent in our cDNA clone). Similarly to CARDs and DEDs, the DD is a homotypic interaction module. Sequence comparisons and threading analysis indicates that the DDs of paracaspases are most similar to those seen in proinflammatory/developmental signaling molecules such as myd88, IRAKs, NF-κB subunits p100/p105, and their *Drosophila* counterparts tube and pelle (see supplemental data at www.molecule.org/cgi/content/full/6/4/961/DC1). The paracaspase Ig domains are most similar to the Ig domains from proteins such as titin, heparan sulfate proteoglycan 2 (HSPG2), and the *C. elegans* protein HIM-4 (www.molecule.org/cgi/content/full/6/4/961/DC1).

Metacaspases from yeast and some from plants contain a proline-rich region at their N terminus (Figure 1a). The plant metacaspases can be divided into two subclasses based on the sequence similarity within their caspase-like domain and their overall domain structure. Type I plant metacaspases contain a prodomain that consists of a proline-rich region and a Zn finger motif typical of plant proteins that function in the hypersensitive response pathway such as lsd-1 (see supplemental data at www.molecule.org/cgi/content/full/6/4/961/DC1). Type II plant metacaspases possess no obvious prodomain but have a conserved insertion of approximately

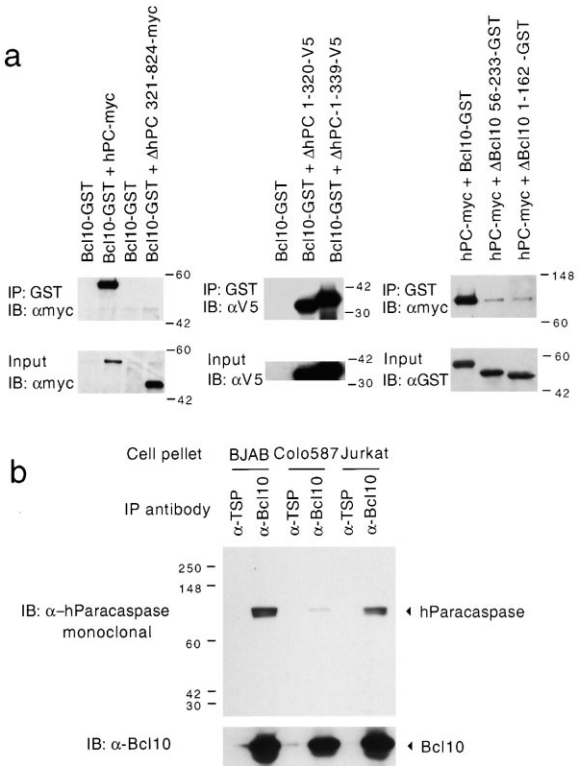

Figure 2. The Human Paracaspase Interacts with Bcl10

(a) Bcl10 immunoprecipitates with human paracaspase. Left panel, Bcl10-GST fusion binds full-length paracaspase but not a truncated version lacking the prodomain (ΔhPC 321-824-myc). Middle panel, Bcl10-GST binds the prodomain of paracaspase. Right panel, Both the N terminus and the C terminus of Bcl10 are required for optimal binding to the full-length paracaspase.

(b) Endogenous interaction between Bcl10 and paracaspase. Precipitation of Bcl10 from BJAB, Colo587, and Jurkat cells pulls down a specific band of 100 kDa that is detected by the human paracaspase monoclonal antibody. Control immunoprecipitations using anti-thrombospondin antibody did not pull down human paracaspase.

180 amino acids between the regions corresponding to caspase p20 and p10 subunits.

Extensive experimental analysis of the human paracaspase has revealed that it does not appear to function as a traditional caspase. Constructs containing full-length, truncated, and artificially oligomerized forms did not induce apoptosis when expressed in mammalian cells. Furthermore, these forms did not appear to undergo autoprocessing, and bacterially expressed, purified forms were unable to cleave a range of known caspase substrates (data not shown).

The Human Paracaspase Interacts with the Oncogene Bcl10

Identification of molecules that bind the prodomains of caspases has illuminated the signaling pathways in which they participate. In order to identify the molecules that may bind and recruit the human paracaspase, we conducted yeast two-hybrid screens using the paracaspase prodomain as bait. Screening of greater than ten million transformants of a Jurkat cell cDNA library

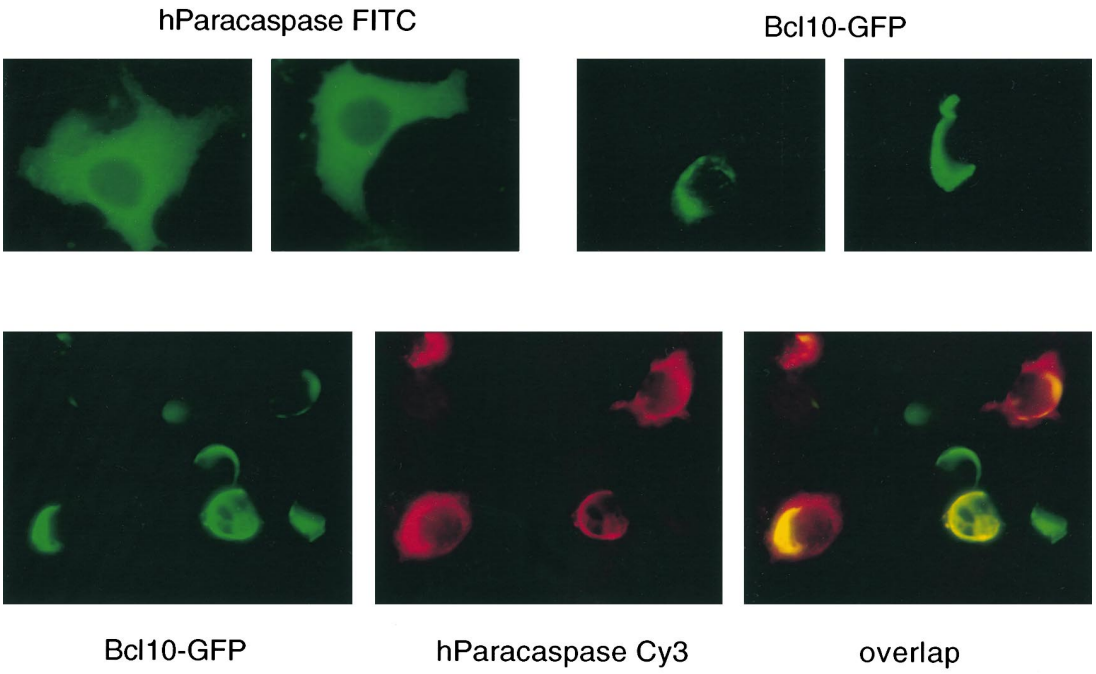

Figure 3. The Human Paracaspase Colocalizes with Bcl10

Subcellular localization and colocalization of human paracaspase and Bcl10. MCF7 cells were transfected with myc-tagged paracaspase and GFP-tagged Bcl10 either separately (upper panels) or together (lower panels). Paracaspase is normally cytoplasmic, whereas Bcl10-GFP localizes to fibrous perinuclear structures. When cotransfected, overlapping of the red and green channels demonstrates that paracaspase specifically colocalizes with Bcl10-GFP.

yielded multiple independent clones encoding the open reading frame of Bcl10.

Bcl10 (c-E10/c-CARMEN/CLAP/CIPER) is the cellular homolog of the equine herpesvirus-2 gene E10. It is a 233 amino acid protein containing an N-terminal CARD domain. Overexpression of full-length and mutant forms of Bcl10 has been shown to weakly activate NF-κB. Notably, the *Bcl10* locus has been found to participate in a translocation event, t(1;14)(p22;q32), frequently associated with MALT lymphoma (Willis et al., 1999).

To examine whether an interaction between Bcl10 and the paracaspase could take place in mammalian cells, we cotransfected epitope-tagged versions of the paracaspase and GST-tagged variants of Bcl10 (Figure 2a). Full-length myc-tagged human paracaspase readily coprecipitated with GST-tagged Bcl10. This interaction appeared to be attributable to the N terminus of the paracaspase, since a paracaspase construct lacking the prodomain (ΔhPC 321-824-myc) was incapable of binding Bcl10, whereas constructs expressing the prodomain alone (ΔhPC 1-320 and ΔhPC 1-339) without the caspase domain effectively bound Bcl10. Bcl10-GST constructs lacking either the amino or carboxyl terminus of Bcl10 (ΔBcl10 56-233-GST and ΔBcl10 1-162-GST) bound substantially less well to the paracaspase than full-length Bcl10, suggesting that both an intact CARD domain and the C terminus are required for this interaction.

To verify whether the Bcl10/paracaspase interaction occurred between endogenously expressed proteins, large numbers of BJAB, Colo587, and Jurkat cells (approximately 10^{11} cells) were lysed and subjected to immunoprecipitation with Bcl10 polyclonal antisera followed by immunoblotting with a monoclonal antibody to the human paracaspase. As shown in Figure 2b, precipitation of endogenous Bcl10 from these lysates resulted in the coprecipitation of endogenous paracaspase.

The Human Paracaspase Colocalizes with Bcl10

Adaptor molecules have been shown to recruit caspases to signaling assemblies through their prodomain. To examine whether Bcl10 was capable of recruiting human paracaspase to a different subcellular location, immunolocalization experiments were conducted (Figure 3). Epitope-tagged human paracaspase gave a diffuse cytoplasmic staining pattern when expressed alone. GFP-Bcl10 has previously been reported to localize to concentrated fibrous perinuclear structures (Yan et al., 1999). Coexpression of both proteins caused the paracaspase to colocalize with the perinuclear Bcl10 staining pattern, confirming the notion that Bcl10 could indeed alter the subcellular localisation of human paracaspase.

The Human Paracaspase/IAP-2 Translocation of MALT Lymphoma t(11;18)(q21;q21) Is Capable of Causing NF-κB Activation

In ongoing database searches for paracaspase homologs, we realized that part of the human paracaspase sequence was present in a chimeric molecule generated by the t(11;18)(q21;q21) translocation of MALT (mucosa associated lymphoid tissue) lymphoma. This translocation creates a chimeric protein that fuses the *cIAP-2(hilp1/MIHC/API2)* gene to what we now know to be the human paracaspase locus (referred to in these papers as *MLT1* (Dierlamm et al., 1999) and *MALT1* (Akagi et al., 1999; Morgan et al., 1999)).

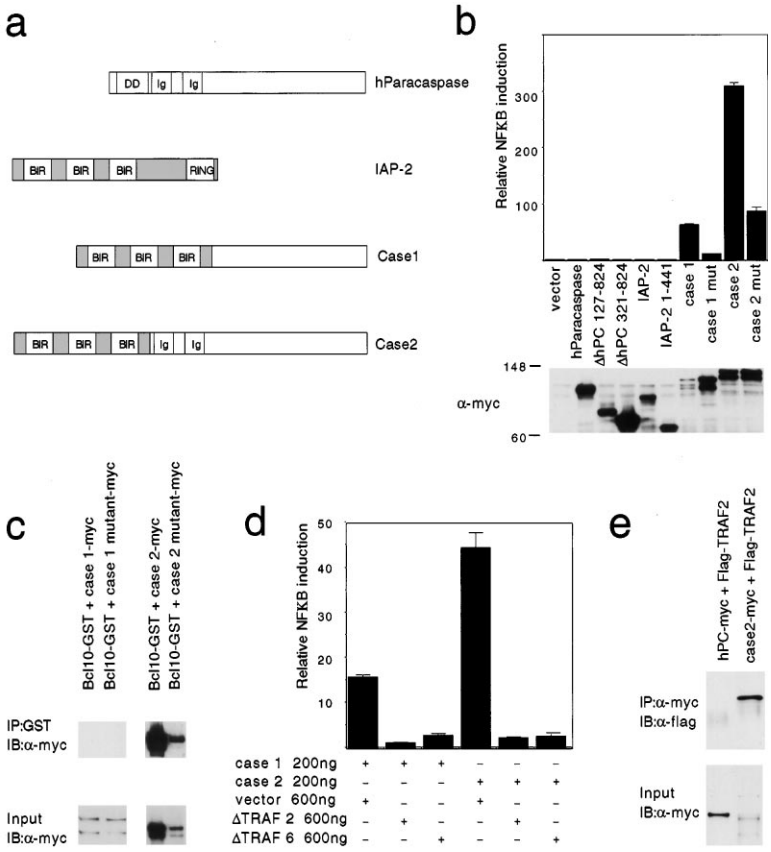

Figure 4. Products of the t(11;18)(q21;q21) IAP-2/Paracaspase Translocation Activate NF-κB Signaling

(a) Domain structure of MALT lymphoma fusion products. In the fusion products, the N-terminal 441 amino acids of IAP-2 are fused to human paracaspase amino acids 324–824 (case 1) or 127–824 (case 2).

(b) MALT lymphoma case 1 and case 2 fusion products activate NF-κB signaling. 293E cells were transfected with plasmids expressing myc-tagged case 1 fusion, case 2 fusion, human paracaspase, IAP-2, and truncated versions of these molecules. Case 1 and case 2 activate expression of NF-κB by 80- and 300-fold, respectively. Cysteine to alanine mutant versions of these constructs are substantially less able to activate NF-κB signaling. Error bars represent the standard deviation of triplicate samples. The experiment was repeated four times, yielding similar results. The data shown is a representative experiment where expression of the transfected gene products was confirmed using an α-myc monoclonal antibody (lower panel Western blot).

(c) MALT lymphoma case 2 fusion but not case 1 fusion binds Bcl10-GST.

(d) Dominant-negative TRAF2 (amino acids 87–501) and dominant-negative TRAF6 (amino acids 289–522) are able to attenuate case 1– and case 2–mediated NF-κB signaling.

(e) TRAF2 binds the case 2 fusion but not full-length paracaspase.

The MALT lymphoma t(11;18)(q21;q21) translocations effectively replace the prodomain of the human paracaspase (either including or excluding the Ig domains) with the three BIR motifs of IAP-2 (Figure 4a). IAPs (inhibitors of apoptosis) are a family of cell death inhibitors capable of preventing death in mammals and insects, possibly through their direct interaction with caspases (LaCasse et al., 1998). Our finding that the human paracaspase binds Bcl10, which is involved in the t(1;14)(p22;q32) translocation, suggests that these proteins may engage a common mechanism in their promotion of MALT lymphoma. Because Bcl10 and the variant forms found in MALT lymphomas have been shown to activate NF-κB, we tested the MALT lymphoma fusion proteins for their NF-κB activation ability.

When overexpressed in 293E(EBNA) cells, the MALT lymphoma case 1 and case 2 fusion products markedly activated transcription from an NF-κB responsive promoter (up to 80-fold for case 1 and 300-fold for case 2). To test whether this response was solely attributable to either the BIR motifs or the paracaspase domain of the fusion, we expressed full-length and truncated versions of these proteins separately. Neither full-length human paracaspase, full-length IAP-2, or the truncated versions of these proteins were able to significantly activate NF-κB (Figure 4b). Western analysis of lysates from this experiment indicate that these full-length and truncated proteins are expressed at levels similar to or higher than the fusion proteins. Thus, both the BIR motifs and paracaspase domain of the chimera are required for the observed NF-κB activation.

We next investigated whether the activation of NF-κB by the case 1 and case 2 fusions was related to the predicted protease activity of the paracaspase domain. Mutation of the catalytic cysteine residue of traditional caspases prevents them from cleaving their substrates. Case 1 and case 2 fusions were constructed in which the conserved catalytic cysteine residue was mutated to alanine. Mutation of the catalytic cysteine markedly reduced NF-κB activation by the fusion proteins, consistent with the hypothesis that the paracaspase portion of the molecule is a cysteine protease (Figure 4b). In both cases, however, a residual amount of NF-κB-activating activity of the mutant fusions was observed, suggesting that they may promote NF-κB activation through more than one mechanism. Alternately, these catalytically inactive fusions may still be able to associate with, recruit, and activate endogenous paracaspase molecules.

The case 1 and case 2 fusions differ in that the case 2 transcript contains the exons encoding the prodomain Ig motifs (Figure 4a). Because Bcl10 binds the paracaspase through its prodomain, we examined whether the case 1 and case 2 fusions were also able to bind Bcl10. As expected, the case 2 fusion (both wild-type and mutant) was capable of being immunoprecipitated with GST-tagged Bcl10 while the case 1 fusion (wild-type and mutant) was not (Figure 4c). Thus, the difference in these proteins' ability to activate NF-κB correlates with their ability to bind Bcl10.

Both Bcl10 and the IAP-2 BIRs have been reported to interact with TRAF2. To investigate whether the MALT lymphoma fusions were activating NF-κB signaling via their assoication with TRAFs, we cotransfected the fusions with dominant-negative forms of TRAFs 2 and

6. Both dominant-negative TRAFs were able to inhibit signaling by the fusions (Figure 4d). Furthermore, TRAF2 was precipitated with the MALT lymphoma case 2 fusion but not full-length paracaspase (Figure 4e). These data are consistent with a model whereby case 1 and case 2 signaling might be dependent upon members of the TRAF adaptor family.

Discussion

The ability of the MALT lymphoma fusions to activate NF-κB signaling suggests a mechanism for their oncogenic effect. Activation of NF-κB signaling either through mutation of rel genes and their upstream regulators or by infection with viral oncogenes has been implicated in a range of hematopoietic tumor types (reviewed in Rayet and Gelinas, 1999). The *IAP-2* gene is known to be NF-κB responsive (Chu et al., 1997), raising the possibility that the t(11;18)(q21;q21) fusion product may feed back to upregulate its own expression.

A role for NF-κB signaling in MALT lymphoma might suggest novel treatments and clarify the mode of action of current treatments. Thus, drugs such as known anti-inflammatories and immunosuppressants that have been shown to inhibit NF-κB signaling in vivo (reviewed in Epinat and Gilmore, 1999) may warrant investigation as treatments. Tetrapeptide inhibitors of caspases have been effectively demonstrated to inhibit caspase activity in vivo, raising the possibility of using equivalent specific peptide inhibitors of the paracaspase to treat MALT lymphoma.

Bcl10 and the human paracaspase are both involved in separate MALT lymphoma translocations and were shown to interact and colocalize within the cell, suggesting a common mode of action. Bcl10 has previously been shown to activate NF-κB signaling. The Bcl10 t(1;14)(p22;q32) translocation of MALT lymphoma usually occurs after the t(11;18)(q21;q21) event and correlates with a more advanced form of the malignancy (Spencer, 1999). Cotransfection of Bcl10 with the case 1/case 2 fusion products in 293 cells gave a mild additive enhancement of NF-κB signaling over that seen from case1/case2 alone (data not shown). We speculate that the t(1;14)(p22;q32) translocation may act to enhance NF-κB signaling beyond a certain threshold, allowing for progression of MALT lymphoma from low-grade to high-grade status.

Comparison of the crystal structure of gingipain R with the caspase structure demonstrates notable structural similarity that, in spite of the limited sequence conservation, suggests a common origin of these proteases. Thus, it appears that the caspase/paracaspase/metacaspase superfamily has emerged early in eukaryotic evolution as an offshoot of a larger, more ancient class of cysteine proteases that also includes such families of cysteine proteases as legumains and hemoglobinases. The peculiarity of the phyletic distribution of the three families of caspase-like proteases is that caspases are so far limited to metazoa, paracaspases are seen in metazoa and *Dictyostelium*, whereas metacaspases are highly conserved in plants and fungi but conspicuously missing in metazoa. This distribution suggests that metacaspases are likely to most closely resemble the ancestral protease present in ancestral eukaryotes. Subsequent evolution could have involved a duplication resulting in the progenitors of the caspase and paracaspase families early in the evolution of the *Dictyostelium*-metazoa lineage, followed by rapid divergence, presumably due to functional diversification. An analysis of the bacterial members of this protease superfamily suggests a specific relationship with the metacaspases of eukaryotes. Metacaspases were also detected in *Trypanosoma* and *Plasmodium*, suggesting that this is the ancient form with a complex history of horizontal gene exchange with the bacteria.

Type I plant metacaspase prodomains contain a C2C2 Zn finger typically seen in proteins such as lsd-1 that mediate the plant hypersensitive response, considered the plant equivalent of programmed cell death. Similar Zn finger modules are also found fused to the *Arabidopsis* ortholog of the *Drosophila* strawberry notch (sno) gene product and yeast ubiquitin ligase. The sno ortholog, which encodes a divergent SWI/SNF family ATPase, is positioned on *Arabidopsis* chromosome 1 next to a cluster of four metacaspase genes. The closest plant homologs of the metazoan caspase activators ced-4 and APAF1 are predicted ATPases of the AP (apoptotic) ATPase family involved in the hypersensitive response. This homology supports the notion that the death signaling pathways of metazoans and the hypersensitive response of plants have a common origin (Aravind et al., 1999). Stress-induced caspase activity in plants and prevention of programmed cell death associated with plant hypersensitive response by caspase inhibitors have been reported (del Pozo and Lam, 1998). It remains to be seen whether these effects are exerted on metacaspases described here or other yet undetected plant members of the caspase-like superfamily.

NF-κB signaling, hypersensitive response, and programmed cell death are diverse mechanisms; however, a common thread to all three is that they are all in some cases employed as stress responses. As such, it is attractive to speculate that the common ancestor of the caspase/paracaspase/metacaspase superfamily may have played a role in stress response pathways in early eukaryotes. The subsequent divergence of these molecules throughout evolution may reflect a demand for specific responses to increasingly diverse environmental stresses and the involvement of programmed cell death in the developmental pathways of multicellular eukaryotes.

Experimental Procedures

Cloning of Paracaspase cDNAs

The *H. sapiens* and *D. reriro* paracaspase cDNAs were cloned from a human fetal kidney library and a zebrafish embryonic library, respectively. The *D. discoideum* cDNA clone was provided by Dr. Takahiro Morio (University of Tsukuba). A *C. elegans* cDNA corresponding to ORF F22D3.6 was PCRed from a mixed-stage cDNA library.

Sequence Analysis and 3D Modeling

Searches of the nonredundant protein sequence database at the National Center for Biotechnology Information (NIH, Bethesda) were performed using the PSI-BLAST program (Altschul et al., 1997). The database of expressed sequence tags (dbEST) was searched using the TBLASTN program (Altschul et al., 1997). Adjustments to the

multiple sequence alignment constructed by using CLUSTAL W (Thompson et al., 1994) were made based on the structure-based alignment performed by superimposing the structures of caspase-1, caspase-3, and gingipain R. 3D modeling of caspase domains and death domains was performed by using a threading approach (ProCeryon, ProCeryon Biosciences Inc.).

Immunoprecipitations

293T cells were transfected with GST-tagged Bcl10 and myc-tagged human paracaspase expression constructs. GST fusion proteins were precipitated from cell lysates using glutathione-agarose beads. For endogenous immunoprecipitations, 10^{11} BJAB, Colo587, or Jurkat cells were lysed and incubated with 100 μg of Bcl10 antisera (Santa Cruz) and 50 μl of protein G beads.

Immunofluorescence

MCF7 cells were plated on LabTek 2-well glass chamber slides and transfected with constructs expressing myc-tagged human paracaspase and/or Bcl10-GFP. Cells were stained with α-myc monoclonal 9E10 (Biomol) primary antibody and FITC (Sigma) or Cy3 (Jackson Immunoresearch) α-mouse secondary antibody.

NF-κB Luciferase Assay

293E cells were transfected with 0.8 μg of expression construct(s) + 0.18 μg pLam3 (NF-κB-responsive luciferase) + 0.02 μg pR-TK (control luciferase). Twenty-four hours posttransfection, luciferase activity was measured using the Dual-Luciferase Reporter Assay System (Promega).

Acknowledgments

We thank monoclonal antibody production, sequencing core, Wenlu Li, Gilbert-Andre Keller, and Jeff Hooley for microscopy, Charlie Eigenbrot for preliminary modeling of the paracaspase, and Takahiro Morio, Guy Salvesen, Henning Stennicke, Jowita Mikolajczyk, James Lee, and members of the Dixit lab for discussions, advice, and reagents.

Received May 25, 2000; revised August 17, 2000.

References

Akagi, T., Motegi, M., Tamura, A., Suzuki, R., Hosokawa, Y., Suzuki, H., Ota, H., Nakamura, S., Morishima, Y., Taniwaki, M., and Seto, M. (1999). A novel gene, MALT1 at 18q21, is involved in t(11;18)(q21;q21) found in low-grade B-cell lymphoma of mucosa-associated lymphoid tissue. Oncogene *18*, 5785–5794.

Altschul, S.F., Madden, T.L., Schaffer, A.A., Zhang, J., Zhang, Z., Miller, W., and Lipman, D.J. (1997). Gapped BLAST and PSI-BLAST: a new generation of protein database search programs. Nucleic Acids Res. *25*, 3389–3402.

Aravind, L., Dixit, V.M., and Koonin, E.V. (1999). The domains of death: evolution of the apoptosis machinery. Trends Biochem. Sci. *24*, 47–53.

Chen, J.M., Rawlings, N.D., Stevens, R.A., and Barrett, A.J. (1998). Identification of the active site of legumain links it to caspases, clostripain and gingipains in a new clan of cysteine endopeptidases. FEBS Lett. *441*, 361–365.

Chu, Z.L., McKinsey, T.A., Liu, L., Gentry, J.J., Malim, M.H., and Ballard, D.W. (1997). Suppression of tumor necrosis factor-induced cell death by inhibitor of apoptosis c-IAP2 is under NF-kappaB control. Proc. Natl. Acad. Sci. USA *94*, 10057–10062.

Cohen, G.M. (1997). Caspases: the executioners of apoptosis. Biochem. J. *326*, 1–16.

del Pozo, O., and Lam, E. (1998). Caspases and programmed cell death in the hypersensitive response of plants to pathogens. Curr. Biol. *8*, 1129–1132.

Dierlamm, J., Baens, M., Wlodarska, I., Stefanova-Ouzounova, M., Hernandez, J.M., Hossfeld, D.K., De Wolf-Peeters, C., Hagemeijer, A., Van den Berghe, H., and Marynen, P. (1999). The apoptosis inhibitor gene API2 and a novel 18q gene, MLT, are recurrently rearranged in the t(11;18)(q21;q21) associated with mucosa-associated lymphoid tissue lymphomas. Blood *93*, 3601–3609.

Eichinger, A., Beisel, H.G., Jacob, U., Huber, R., Medrano, F.J., Banbula, A., Potempa, J., Travis, J., and Bode, W. (1999). Crystal structure of gingipain R: an Arg-specific bacterial cysteine proteinase with a caspase-like fold. EMBO J. *18*, 5453–5462.

Epinat, J.C., and Gilmore, T.D. (1999). Diverse agents act at multiple levels to inhibit the Rel/NF-kappaB signal transduction pathway. Oncogene *18*, 6896–6909.

LaCasse, E.C., Baird, S., Korneluk, R.G., and MacKenzie, A.E. (1998). The inhibitors of apoptosis (IAPs) and their emerging role in cancer. Oncogene *17*, 3247–3259.

Morgan, J.A., Yin, Y., Borowsky, A.D., Kuo, F., Nourmand, N., Koontz, J.I., Reynolds, C., Soreng, L., Griffin, C.A., Graeme-Cook, F., et al. (1999). Breakpoints of the t(11;18)(q21;q21) in mucosa-associated lymphoid tissue (MALT) lymphoma lie within or near the previously undescribed gene MALT1 in chromosome 18. Cancer Res. *59*, 6205–6213.

Morio, T., Urushihara, H., Saito, T., Ugawa, Y., Mizuno, H., Yoshida, M., Yoshino, R., Mitra, B.N., Pi, M., Sato, T., et al. (1998). The Dictyostelium developmental cDNA project: generation and analysis of expressed sequence tags from the first-finger stage of development. DNA Res. *5*, 335–340.

Rayet, B., and Gelinas, C. (1999). Aberrant rel/nfkb genes and activity in human cancer. Oncogene *18*, 6938–6947.

Spencer, J. (1999). Aggressive mucosa associated lymphoid tissue lymphomas are associated with mutations in Bcl10. Gut *44*, 778–779.

Thompson, J.D., Higgins, D.G., and Gibson, T.J. (1994). CLUSTAL W: improving the sensitivity of progressive multiple sequence alignment through sequence weighting, position-specific gap penalties and weight matrix choice. Nucleic Acids Res. *22*, 4673–4680.

Willis, T.G., Jadayel, D.M., Du, M.Q., Peng, H., Perry, A.R., Abdul-Rauf, M., Price, H., Karran, L., Majekodunmi, O., Wlodarska, I., et al. (1999). Bcl10 is involved in t(1;14)(p22;q32) of MALT B cell lymphoma and mutated in multiple tumor types. Cell *96*, 35–45.

Yan, M., Lee, J., Schilbach, S., Goddard, A., and Dixit, V. (1999). mE10, a novel caspase recruitment domain-containing proapoptotic molecule. J. Biol. Chem. *274*, 10287–10292.